Size-resolved chemical composition of the September 2009 Sydney dust storm

M. Radhi, M. A. Box, G. P. Box, and D. D. Cohen

ABSTRACT

In September 2009, a major dust storm crossed eastern Australia, blanketing Sydney on two occasions. We collected size-resolved aerosol samples on both days, and also on the following days, for comparison. The size distribution during the dust storm showed a strong coarse mode, as expected. We subjected these samples to Ion Beam Analysis at ANSTO, obtaining their size-resolved chemical composition. In this paper we present these results, and compare them with some of the analysis of similar samples obtained in field trips to the Lake Eyre Basin of central Australia, the source region for much of the dust. In particular, the Fe/Al ratios (~0.9) are similar to LEB values (~0.8-1.0), and higher than northern hemisphere values (~0.55). Salt entrainment indicates a contribution from dry lakes.

Keywords: dust storm, ion beam analysis, mineral aerosol, size-resolved chemistry.

INTRODUCTION

On 23 September 2009, a major dust storm passed across most of eastern Australia, reaching Sydney in the early hours of the morning. A second, smaller storm occurred on 26 September. For a satellite view of some of the environmental impacts of the first storm, see Jones and Christopher (2010).

The Sydney basin is home to around 4 million people, and some significant industry. It is largely enclosed, so for the most part its air pollution, including particulates, is locally generated, and dominated by secondary sulfates and sea salt (in summer), smoke (in winter), plus auto emissions. Occasional long range transport brings rural dust to the region (Cohen *et al.* 2010).

We used a 12 stage Micro Orifice Uniform Deposition Impactor (MOUDI) (Marple *et al.* 1991) to collect size-segregated aerosol samples during the two dust storm events, and also on the day after, for comparison purposes. During the first dust storm (and the following day) the MOUDI was deployed on the roof of the Physics building at the University of New South Wales (close to the coast), while during the second dust storm (and the following day) the MOUDI was deployed in the backyard of a house in the west of Sydney. Sampling times varied according to ambient dust levels (Table 1).

These samples have been analysed for elemental composition using Ion Beam Analysis (IBA) in a similar manner to samples collected in a series of field trips we have undertaken to the Lake Eyre Basin. We compare results to determine whether this area is the likely source of the dust.

METHODS

The MOUDI allows identification of any compositional differences between particles of different size. The sum of the masses on all MOUDI substrates can be considered a good measurement of Total Suspended Particulates in the atmosphere (TSP) for one sampling period, as all particles for different sizes are collected from the same parcel of air. The collection and analysis protocols are the same as we employed in three field trips to sites in the Lake Eyre Basin (LEB) (Radhi *et al.* 2009, 2010; Radhi 2010), and it is our intention when all analyses are complete to make a thorough comparison of all four data sets.

The MOUDI has stage cuts at 18.0, 10.0, 5.6, 3.2, 1.8, 1.0, 0.56, 0.32, 0.18, 0.1 and 0.056 μm aerodynamic diameters, plus an after filter (< 0.056 μm). This allows identification of any compositional differences between particles of different size, as the aerosols in many locations are known to be chemically variable, with significant differences between fine (mostly secondary) and coarse (mostly primary) modes (d'Almeida *et al.* 1991). The inlet to the MOUDI consisted of two stainless steel bowls with a 2 cm gap between them to allow omnidirectional sampling, while its flow rate was 30 l min^{-1}.

The collection substrates used on the first 11 stages (inlet to stage 10) were polycarbonate Isopore filters, 47 mm in diameter with 0.8 μm pore size. The final stage (stage 11) substrate was a Teflon-backed Fluoropore filter, 47 mm in diameter with 1 μm pore size. We weighed the substrates before and after sampling at the Australian Nuclear Science and Technology Organization (ANSTO) using a Mettler Toledo MX5 balance with repeatability 0.0008 mg at gross load. The temperature during the weighing process was 22 ± 1.5 °C, and the humidity was 50 ± 5%. This provided the gross particulate loading on each filter.

The substrates were then analysed using accelerator-based IBA techniques, Proton-Induced X-ray Emission (PIXE) and Proton-Induced Gamma-ray Emission (PIGE), at ANSTO (Cohen 1993, 1998; Cohen *et al.* 1996). Cohen *et al.* (2002) discuss in detail the minimum detection limits and errors related to PIXE and PIGE measurements, which are around 10% for major elements. The IBA technique uses an 8 mm diameter beam of 2.6 MeV protons with 10-15 nA target current. As the spatial distribution of sample on each substrate varied, and the ion

Table 1. Timings of sample collection and TSP mass concentrations (μg m^{-3}).

Collection	Start		End		Total hours	TSP
	Date	Time	Date	Time		
1st Dust Storm	23/09/2009	9:06:00	23/09/2009	14:32:00	5:26:00	578
Day After	23/09/2009	15:00:00	24/09/2009	13:36:00	22:36:00	33
2nd Dust Storm	26/09/2009	5:50:00	27/09/2009	5:00:00	23:10:00	58
Day After	27/09/2009	8:12:00	28/09/2009	7:25:00	23:13:00	25

beam only sampled the central 10% of the impacted area of the filter. We have used the IBA results, primarily, to obtain the ratio of elements to the most abundant element in our samples.

GRAVIMETRIC MASS DISTRIBUTIONS

During the first dust storm to hit Sydney the (time averaged) sampled TSP was 578 μg m^{-3}, reducing to 33 μg m^{-3} the day after the dust storm (see Table 1). The size-resolved mass concentrations during the dust storm day and the day after are presented in Figure 1. It is clear from this graph that the mass size distribution during the dust storm has a broad peak in the coarse fraction, with 81% of the TSP in this fraction. We define the fine fraction to correspond to PM2.5, and the course fraction to be all larger particles. PMn is defined as 'particulate matter with aerodynamic diameters less than n microns'. During the day after the dust storm the size distribution has a peak in the coarse fraction, but this fraction comprised only 59% of the TSP.

We have previously collected size-resolved samples during both dust storm and quiescent conditions at different sites within the LEB: Birdsville Qld (Radhi *et al.* 2009); Muloorina SA (Radhi *et al.* 2010); and Fowlers Gap Station (FGS) NSW (Radhi 2010). These locations are shown in Figure 2. The LEB is the major dust source region in Australia, and one of the largest in the Southern Hemisphere (Prospero *et al.* 2002; McTainsh and Lynch 1996; Bullard *et al.* 2008), and is where much of the storm dust is believed to have originated (G. McTainsh, private communication).

To contrast between the behaviour of the mass size spectrum for several of these dust storms we applied a smoothing/inversion procedure (Keywood *et al.* 1999), to the Sydney, Birdsville (a weak storm), Muloorina and FGS data, for both the first dust storm day, and the day after. (This is a non-linear iterative inversion procedure based on the MOUDI transmission kernels, starting from an initial guess. Uncertainties can only be estimated, but are probably ~5–10%.) These results are presented in Figure 3, and summarised in Table 2. It is clear from these results that the coarse mode dominates during the dust storm event but the mass diameter peaks are variable, depending on how strong the dust storm was, and how far away is the sampling site from the dust sources. The day after the dust storm the PM1 fraction contributed around 28%, 14%

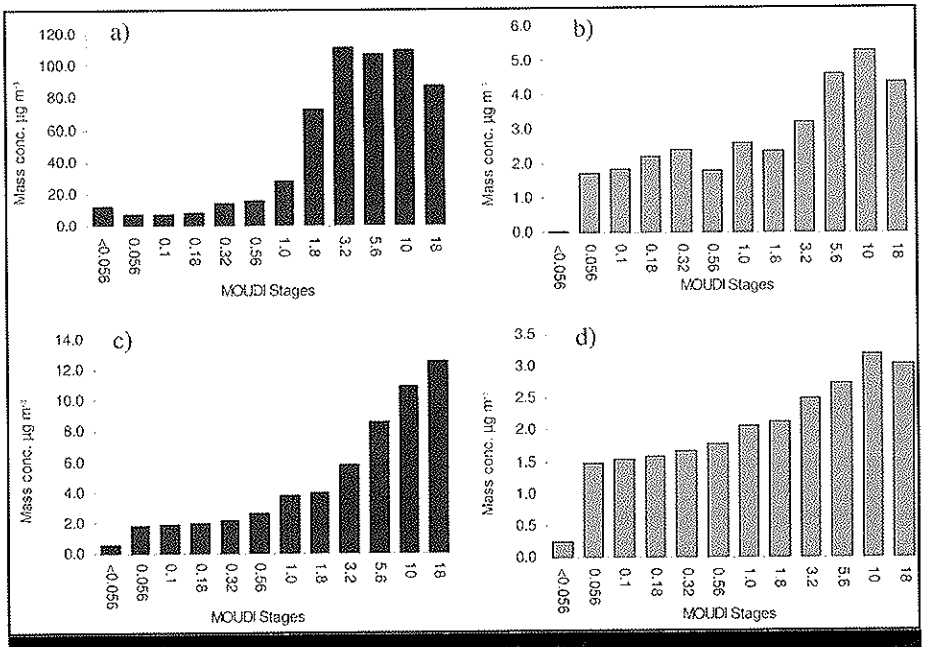

Figure 1. Size-resolved mass distributions of (a) first dust storm; (b) day after first dust storm; (c) second dust storm; (d) day aftersecond dust storm.

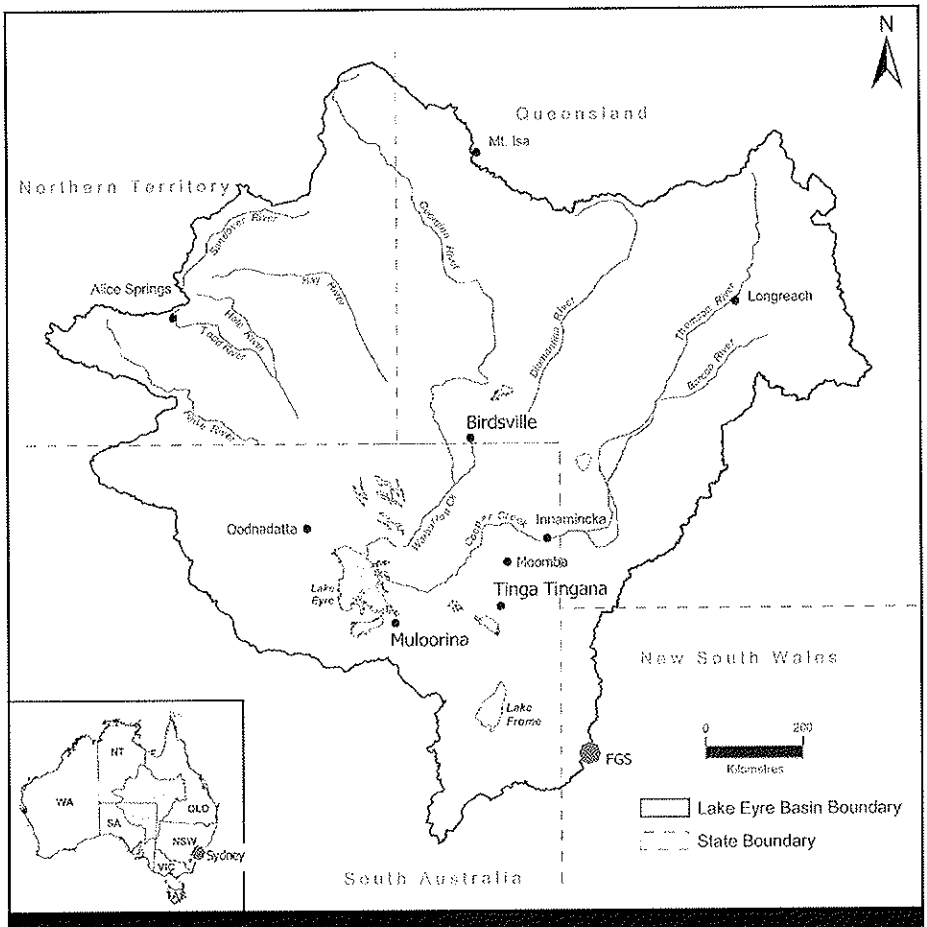

Figure 2. Map of the Lake Eyre Basin, showing Birdsville, Muloorina, Fowlers Gap Station (FGS), and Sydney.

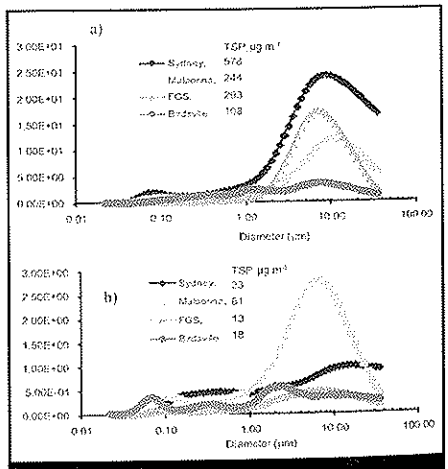

Figure 3. a) Size-resolved mass concentrations sampled during first dust storms at Sydney, Muloorina and FGS. b) Size-resolved mass concentrations sampled during the day after dust storms at Sydney, Muloorina and FGS.

Table 2. Mass size fractions for Sydney first dust storm day and the day after, comparing with mass size fractions (MSF) during dust storms at LEB sites.

MSF ($\mu g\ m^{-3}$) or ratio	First Dust Storm Day				Day After			
	Sydney	Muloorina	FGS	Birdsville	Sydney	Muloorina	FGS	Birdsville
TSP	579	244	293	108	33	61	13	18
PM1	55	22	11	29	9	9	2	6
PM2.5	109	39	33	47	14	17	4	9
PM10	353	142	204	84	23	47	10	14
PM2.5/TSP	19%	16%	11%	44%	41%	28%	33%	53%
PM1/PM2.5	51%	56%	33%	62%	70%	51%	53%	60%
PM1/TSP	10%	9%	4%	27%	28%	14%	18%	32%

Table 3. Ratios of elements to Si.

Element	First Dust	Day after	Second Dust	Day after	Crust
Na	3.38E-02	3.18E-01	1.49E-01	6.77E-01	8.37E-02
Al	3.53E-01	2.99E-01	3.28E-01	3.00E-01	2.92E-01
P	5.67E-04	1.06E-02	3.39E-03	1.33E-02	3.72E-03
S	7.70E-03	8.81E-02	3.15E-02	1.48E-01	1.24E-03
Cl	3.19E-03	7.70E-02	6.30E-02	4.05E-01	5.14E-04
K	1.09E-01	7.24E-02	9.09E-02	6.89E-02	7.41E-02
Ca	5.19E-02	6.52E-02	6.27E-02	5.83E-02	1.47E-01
Ti	3.18E-02	2.15E-02	2.78E-02	1.75E-02	2.00E-02
V	1.02E-03	4.71E-04	1.63E-04	3.27E-04	4.26E-04
Cr	6.33E-04	9.42E-03	6.77E-03	6.22E-03	3.62E-04
Mn	6.26E-03	6.95E-03	6.12E-03	9.01E-03	3.37E-03
Fe	3.12E-01	2.87E-01	3.20E-01	2.47E-01	2.00E-01
Co	2.07E-03	1.77E-03	1.14E-03	1.80E-03	8.87E-05
Ni	1.61E-04	5.53E-03	3.06E-03	4.75E-03	2.98E-04
Cu	3.98E-03	3.06E-03	2.28E-03	2.13E-03	2.13E-04
Zn	1.45E-03	4.12E-03	2.90E-03	3.93E-03	2.48E-04
Br	1.23E-04	3.18E-03	1.59E-03	5.40E-03	8.51E-06
Sr	6.90E-04	2.36E-04	8.98E-04	3.44E-03	1.31E-03
Pb	3.69E-04	1.77E-03	1.18E-03	1.15E-03	5.32E-08
Cl/Na	9.46E-02	2.42E-01	4.24E-01	5.99E-01	6.14E-03
Fe/Al	8.83E-01	9.61E-01	9.75E-01	8.22E-01	6.84E-01

Table 4. Slopes of scatter plots vs. Si, with [correlation coefficient]

Element	Sydney	Birdsville	Muloorina	FGS
Fe	0.32 [0.99]	0.23 [0.98]	0.31 [0.99]	0.35 [0.94]
Al	0.36 [1.0]	0.30 [0.99]	0.32 [0.99]	0.36 [0.97]
Ti	0.033 [0.99]	0.026 [0.97]	0.025 [0.99]	0.028 [0.99]
Ca	0.056 [0.96]	0.066 [0.97] (0.034) [0.73]	0.18 [0.94]	0.10 [0.96]
Mn	0.064 [0.94]	0.0033 [0.94]	0.0029 [0.96] (0.0015) [0.92]	0.0086 [0.94]
K	0.11 [0.99]	0.053 [0.98]	0.085 [0.99]	0.12 [0.99]

and 18% of the TSP for Sydney, Muloorina and FGS respectively, which indicates that in Sydney, urban/industrial activity may have made a significant (relative) contribution to TSP, on the day after the dust storm, as would be expected. Some larger particles may, of course, have settled out, as the wind speeds were lower.

The second dust storm hit Sydney on 26 September, and the TSP during this period was 58 and 25 $\mu g\ m^{-3}$, for the dust storm day and the day after, respectively. The size-resolved mass concentrations during this period are listed in Figure 1. It is clear from this graph that these two size distributions are reasonably similar to those of the first storm, although reduced in scale, especially during the dust storm itself. The main difference can be seen in the lower coarse mode of the storm sample, which we believe reflects a combination of gravitational settling, plus some coagulation of the larger particles.

ELEMENTAL COMPOSITION

IBA showed that, as expected, Si is an abundant element in all size fractions, and is used in this study, as in our LEB studies, as a dust 'indicator' for Australian desert aerosol (*i.e.* an indicator of natural, rather than anthropogenic, aerosol). The elemental concentrations determined through the IBA are used to calculate the mass ratio of elements to Si: these ratios are summarised in Table 3, along with the global average mass ratios of these elements in the Earth's crust from CRC Handbook (Lide 1997). Size-resolved mass ratios for selected elements are presented in Figure 4. We have also constructed scatter plots of selected elements vs. Si – see Table 4 – for the two dust storm days (hence comprising 24 data points). The elements are classified into three groups: crustal elements (Al, Fe, Ca, K, Mn and Ti); salt (Na and Cl); and others.

ANSTO has been collecting PM2.5 samples in Sydney for many years (on Sundays and Wednesdays), and subjecting them to similar IBA processing. Their results show that their 'soil' category contributes 5% to 15% of PM2.5, with various 'industrial' (including transport) contributions being more important (see the Monthly Summary Sheets link at http://www.ansto.

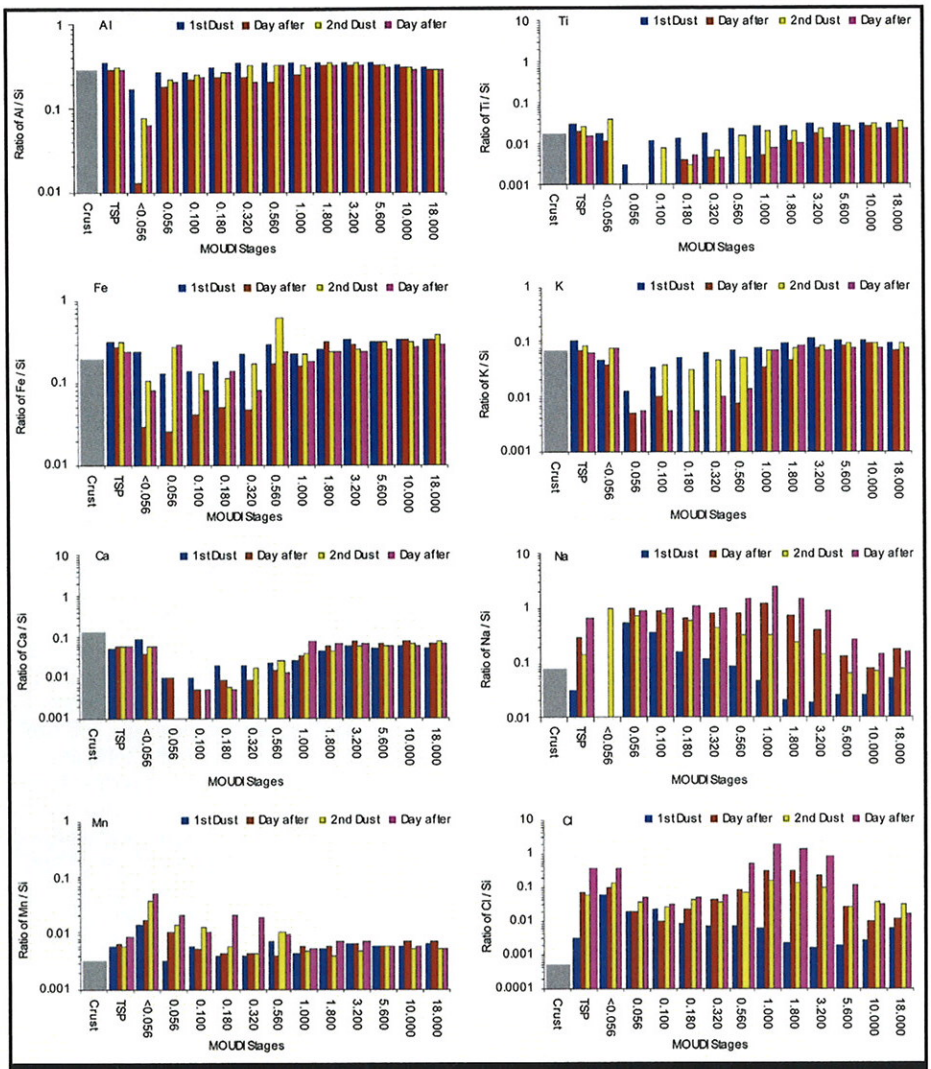

Figure 4. Ratios of some elements to Si over all stages collected by the MOUDI.

gov.au/environment/iba).

Crustal elements

The size-resolved mass ratios in Figure 4 show that Al occurred in most size fractions. By contrast with the crustal value, the Al/Si mass ratios were moderately higher during dust storm days, but close to the crustal value during the days after the dust storms. The Ti/Si mass ratio plot shows that Ti is predominately in the upper fine and coarse fractions in all events. The TSP Ti/Si mass ratios were high during dust storm days by contrast with the crustal value and are consistent with the values found in the LEB during dust activities. Nevertheless this ratio is close to the crustal value during the days after the dust storms.

It is clear from the size-resolved mass ratios in Figure 4 that the Fe/Si mass ratio is largest in the coarse fraction in all events. During the first dust storm the Fe/Si TSP ratios were 0.312 and 0.287, and during the second dust storm they were 0.32 and 0.247, for the dust storm day and day after, respectively. These ratios are consistent with the values we found at various locations within the LEB (Radhi *et al.* 2009, 2010). In turn, the Fe/Al mass ratios were in the range between ~0.8-1.0, which is again consistent with the values found at LEB locations and is higher than values found during dust storms over Northern Hemisphere sites such as Beijing, China (0.55-0.6, Sun *et al.* 2005), and Niger (0.43, Lafon *et al.* 2006). This is a reflection of the more reddish nature of Australian desert soils, compared with northern hemisphere deserts.

Qin and Mitchell (2009) have performed a cluster analysis of ground-based remote sensing data from a range of sites around Australia, including Birdsville. They have derived four classes, which they identify as aged smoke, fresh smoke, coarse dust, and a 'super-absorptive' class of unknown origin. Their coarse dust class has significant absorption in the blue spectral region, which points to a high hematite content. This, again, is consistent with our analysis.

Ca is found mainly in the upper fine and coarse fractions in all events, with the TSP Ca/Si mass ratios lower than the crustal value, which is consistent with what has been found at LEB sites. The Mn/Si mass ratio was dominated by the fine fraction as shown in the size-resolved plot. This ratio was high in all samples by contrast with the crustal value, but is consistent with values found at the LEB sites.

The size-resolved K/Si mass ratios were close to crustal in (almost) all size fractions during the dust storm days, but predominated in the coarse fraction during the day after the dust storm. The K/Si TSP ratio was higher than the crustal value during the dust storm days but close to this value during the day after. It has been found at FGS during a dust storm this ratio was 0.12, which is close to the value of 0.11 found during the first day dust storm.

In Table 4 we compare the slopes and regression coefficients of scatter plots of these six elements for each site. (In some cases the scatter plots showed two populations, and the second slope is included in brackets, when the correlation was good. In the case of Ca data from Birdsville, the second population could be traced to air having passed over gypsum-rich areas (Radhi *et al.* 2010)). These results show that the Fe/Si and Al/Si ratios are consistent with the Muloorina and Fowlers Gap results, slightly more than with Birdsville. (Note that Fowlers Gap is on the edge of the LEB, and downwind of the major source regions). The other ratios may be said to be broadly consistent, given the variability of those ratios across the LEB sites.

Na and Cl

The size-resolved mass ratios of Na/Si in Figure 4 show a different structure for each sample. During the first dust storm day this pattern was bimodal with a strong ultrafine peak, a minimum in the 1.8-3.2 μm range, and then a secondary peak at 18.0 μm. During the second dust storm this distribution was unimodal with a peak in the fine fraction, and reducing steadily but remaining larger than for the first storm. The day after the dust storm the Na/Si distribution shows a comparable pattern for both samples, with high values in the fine fraction and a weak peak in the 1.0-3.2 μm range, and lower values in the coarse fraction. The Na/Si TSP mass ratios are higher than 0.083, the value in the Earth's crust, for all samples excluding the first dust storm sample (0.033) (presumably a reflection of the higher dust concentration on that day), and this feature has been reported by Radhi *et al.* (2010) during dust storm events at Muloorina, and also FGS.

Cl occurred in all size fractions for all events as shown in Figure 4. It is clear from this Figure that the Cl/Si pattern follows the Na/Si pattern during the first dust storm day, while for the rest of the samples this pattern has a broad peak in the 1.0-3.2 μm range. The TSP Cl/Si mass ratios were higher than the value in the Earth's crust in all samples which indicates that non-crustal sources have contributed to the total Cl in all events. The Cl/Si mass ratio during the first dust storm is close to the value found at Muloorina and FGS sites during dust storm activities (Radhi *et al.* 2010), which suggested the uplift of

halite from the surrounding dry lakes.

The TSP Cl/Na mass ratios were higher than the crustal ratio in all samples (Table 3), though still lower than 1.8, the seawater value. During the first dust storm this ratio was very close to the value found at Muloorina during non-dust days, which reflected the influence of dry salt from Lake Eyre. In the other samples the high Cl/Na ratio is indicative of a contribution from another source (such as sea spray) to total salt found in these samples. Note that in the presence of sulfuric acid gas, the Cl^- ion may be displaced by SO_4^{2-}, reducing the Cl/Na ratio (Radhi *et al.* 2009).

Scatter plots of Na vs. Si, and Cl vs. Si showed no obvious correlations, except for the first dust storm day, which is shown in Figure 5. These results are consistent with a mostly non-crustal source for these elements. Scatter plots of Cl vs. Na were far more interesting, revealing (at least) two populations. Figure 5 shows scatter plots of Cl vs. Na for the first dust storm day, the second dust storm day, and the two days after (combined). The first dust storm day is clearly the odd one out. For the other three days, we see a good correlation, with a slope close to 1.0, plus a Na offset. These results may be interpreted as a NaCl population (but with the Cl depleted by airborne reactions), plus another Na source, presumably crustal.

By contrast, the scatter plot for the first dust storm day shows a slope around 0.1, and little or no offset, suggesting a primarily crustal source for both. The Na vs. Si plot for this day alone shows a reasonable correlation, plus an offset. Taken together, these results suggest two Na sources for this sample, crustal, and halite. In our LEB studies, we found that the salt fraction actually decreased during strong dust storms (Radhi *et al.* 2010), suggesting that the winds responsible were more able to loft soil fragments than salts. A similar conclusion presumably applies to the first dust storm.

Others

The TSP mass ratios of S, Cr, Co, Ni, Cu, Zn, Br and Pb to Si were higher than the crustal values for all samples (Table 3) and these elements occurred in most size fractions. These values are consistent with the values found at the LEB sites by Radhi *et al.* (2009, 2010). We have produced scatter plots for many of these elements for our various data sets, but the correlations are mostly poor to moderate, and hardly worth presenting here. Partly this is a reflection of the higher IBA uncertainty levels for these trace elements (Cohen *et al.* 2002). In some cases there is evidence of more than one population. These results are consistent with the mineral-rich nature of the region, which contains a number of mines, including open-cut mines, for a range of minerals. Air mass back trajectories were sometimes able to indicate the reasons for concentration differences.

DISCUSSION AND CONCLUSION

The Lake Eyre Basin is a region of dry salt lakes, and a major source of aeolian dust (Greene at al. 2009; McTainsh 1989). Recent drought conditions have increased this dust activity (Mitchell *et al.* 2010). The dust storms which swept across much of eastern Australia in September 2009 blanketing most of the major population centres in New South Wales and Queensland, including Australia's largest city, Sydney, are a dramatic manifestation of these processes. (Some of the dust was probably uplifted from surrounding areas, which have also experienced these conditions).

We have collected size-resolved aerosol samples in order to investigate their chemical composition. The first key finding is that the Fe/Al ratio of ~0.9 is very similar to this ratio at three sites within the Lake Eyre Basin (~0.8-1.0), and around 50% higher than equivalent northern hemisphere values. This is a direct reflection of the high iron (hematite) content of Australian desert soils (not only in the LEB), which are far more reddish than northern hemisphere deserts. Enrichment in Cu, Zn and Pb (among other elements) is also consistent with mining activities in the area.

The Cl/Si mass ratio during the first dust storm was similar to values measured at Muloorina, close to Lake Eyre, a dry salt lake (although currently filling with water), although there appear to be two sources of Na in this sample. For the other three samples, the Cl/Na correlation strongly suggests that halite dominates. This is a clear indication of the entrainment of dry salt along with the dust, giving further support to the suggestion that this region was the source of at least a significant fraction of the dust.

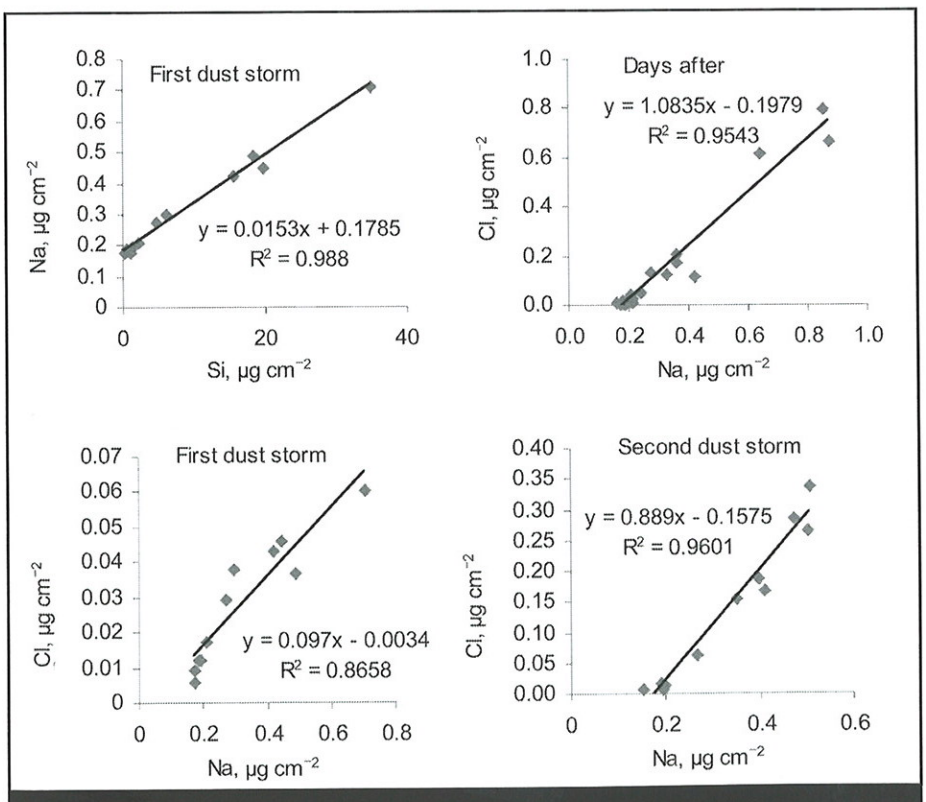

Figure 5. Scatter plots for Na and Si, Na and Cl.

ACKNOWLEDGEMENTS

This work was supported in part by ARC grant DP0451400. Ion Beam Analysis was performed under AINSE grant AINGRA09057. We thank Ed Stelcer for his assistance.

REFERENCES

d'Almeida, G. A., Koepke, P., and Shettle, E. P., 1991, *Atmospheric Aerosols: Global Climatology and Radiative Characteristics*. A. Deepak Publishing, Hampton VA, USA

Bullard, J., Baddock, M., McTainsh, G. H., and Leys, J., 2008, Sub-basin scale dust source geomorphology detected using MODIS. *Geophysical Research Letters*, **35**, L15404.

Cohen, D. D., 1993, Applications of simultaneous IBA techniques to aerosol analysis. *Nuclear Instruments and Methods in Physics Research Section B: Beam Interactions with Materials and Atoms*, **79**, 385-388.

Cohen, D. D., 1998, Characterisation of atmospheric fine particles using IBA techniques. *Nuclear Instruments and Methods in Physics Research Section B: Beam Interactions with Materials and Atoms*, **136-138,** 14-22.

Cohen, D. D., Bailey, G. M., and Kondepudi, R., 1996, Elemental analysis by PIXE and other IBA techniques and their application to source fingerprinting of atmospheric fine particle pollution. *Nuclear Instruments and Methods in Physics Research Section*

B: Beam Interactions with Materials and Atoms, **109-110,** 218-226.

Cohen, D. D., Siegele, R., Ivo, O., and Stelcer, E., 2002, Long-term accuracy and precision of PIXE and PIGE measurements for thin and thick sample analyses, *Nuclear Instruments and Methods in Physics Research Section B: Beam Interactions with Materials and Atoms,* **189**, 81– 85.

Cohen, D. D., Stelcer, E., and Crawford, J., 2010, Fine particle characterization, source apportionment and long range dust transport into the Sydney basin: A long term study between 1998 and 2009, *Atmospheric Pollution Research* (accepted).

Greene, R. S., Cattle, S. R., and McPherson, A. A., 2009, Role of eolian deposits in landscape development and soil degradation in southeastern Australia. *Australian Journal of Earth Sciences*, **56**, 55-65.

Jones, T. A. and Christopher, S. A., 2010, Assessment of temperature and humidity changes associated with the September 2009 dust storm in Australia. Submitted to *Geophysical Research Letters.*

Keywood, M. D., Ayers, G. P., Gras, J. L., Gillett, R. W., and Cohen, D. D., 1999, Relationships between size segregated mass concentration data and ultrafine particle number concentrations in urban areas. *Atmospheric Environment,* **33**, 2907-2913.

Lafon, S., Sokolik, I. N., Rajot, J. L., Caquineau, S., and Gaudichet, A., 2006, Characterization of iron oxides in mineral dust aerosols: Implications for light absorption. *Journal of Geophysical Research,* **111**, D21207, doi:10.1029/2005jd007016.

Lide, D. R., 1997, CRC *Handbook of Chemistry and Physics.* CRC Press, Boca Raton, Fl., USA.

Marple, V. A., Rubow, K. L., and Behm, S. M., 1991, A microorifice uniform deposit impactor (MOUDI): description, calibration, and use. *Aerosol Science and Technology,* **14**, 434-446.

McTainsh, G H, 1989, Quaternary aeolian dust processes and sediments in the Australian region. *Quaternary Science Review,* **8**, 235-253.

McTainsh, G. H., and Lynch, A. W., 1996, Quantitative estimates of the effect of climate change on dust storm activity in Australia during the Last Glacial Maximum. *Geomorphology*, **17**, 263-271.

Mitchell, R M, Campbell, S K, and Qin, Y, 2010, Recent increase in aerosol loading over the Australian arid zone. *Atmospheric Chemistry and Physics,* **10**, 1689-1699.

Prospero, J. M., Ginoux, P., Torres, O., Nicholson, S. E., and Gill, T. E., 2002, Environmental characterization of global sources of atmospheric soil dust identified with the NIMBUS 7 Total Ozone Mapping Spectrometer (TOMS) absorbing aerosol product. *Reviews of Geophysics,* **40**, doi:10.1029/2000RG000095.

Qin, Y, and Mitchell, R M, 2009, Characterisation of episodic aerosol types over the Australian continent. *Atmospheric Chemistry and Physics,* **9**, 1943-1956.

Radhi, M., Box, M. A., Box, G. P., Mitchell, R. M., Cohen, D. D., Stelcer, E., and Keywood, M. D., 2009, Optical, Physical and Chemical Characteristics of Australian Continental Aerosols: Result from a Field Experiment. *Atmospheric Chemistry and Physics, Discussions,* **9**, 25085-25125.

Radhi, M, 2010, The Physical and Chemical Properties of Australian Continental Aerosols. Thesis submitted for PhD, University of New South Wales.

Radhi, M., Box, M. A., Box, G. P., Mitchell, R. M., Cohen, D. D., Stelcer, E., and Keywood, M. D., 2010, Size-Resolved Mass and Chemical Properties of Dust Aerosols from Australia's Lake Eyre Basin. *Atmospheric Environment* (accepted).

Sun, Y., Zhuang, G., Wang, Y., Zhao, X., Li, J., Wang, Z., and An, Z., 2005, Chemical composition of dust storms in Beijing and implications for the mixing of mineral aerosol with pollution aerosol on the pathway, *Journal of Geophysical Research,* **110**, D24209, doi:10.1029/2005JD006054.

AUTHOR DETAILS:

Majed Radhi
Research Assistant
School of Physics
University of New South Wales
Sydney NSW 2052 Australia

Michael A. Box
Senior Visiting Fellow
School of Physics
University of New South Wales
Sydney NSW 2052 Australia
Ph 61-2-93854545
Email m.box@unsw.edu.au

Gail P. Box
Visiting Fellow
School of Physics
University of New South Wales
Sydney NSW 2052 Australia

David D. Cohen
Senior Principal Research Scientist
Institute for Environmental Research
Australian Nuclear Science and Technology Organisation
Locked Bag 2001, Kirrawee, NSW, 2232, Australia

EPHC Decisions

Australia's environment ministers made progress on the key issues of waste, heritage and water at the 21st meeting of the Environment Protection and Heritage Council (EPHC) in Darwin on 5 July. Environment ministers also focused on key environmental challenges relating to chemicals and air quality.

The Council decided on five priority areas for 2010 and beyond: air quality, water quality, heritage, waste and chemicals. Harmonisation of environmental regulations for industry, including adoption of common classifications, common methodologies and better coordinated reporting, was also discussed. Other priorities which emerged included the incorporation of indigenous values and management into heritage protection and water quality planning; a collaborative approach to the development of new environment legislation and the need to further investigate the links between climate change, water quality and soil health.

Further information is available from the Communique which can be downloaded from the News page from the EPHC website, www.ephc.gov.au